FORM TI-12
8/94

WAPD-T-3143

CONF-9705119--1
CONF-970701--2

ELECTRICAL AND OPTICAL PERFORMANCE CHARACTERISTICS OF 0.74eV p/n InGaAs MONOLITHIC INTERCONNECTED MODULES

David M. Wilt, NASA Lewis Research Center
Navid S. Fatemi, Essential Research, Inc.
Philip P. Jenkins, Essential Research, Inc.
Victor G. Weizer, NASA Lewis Research Center
Richard W. Hoffman, Jr., Essential Research Inc.
Raj K. Jain, National Research Council
Christopher S. Murray, Bettis Atomic Power Laboratory
David R. Riley, Bettis Atomic Power Laboratory

DE-AC11-93PN38195

BETTIS ATOMIC POWER LABORATORY WEST MIFFLIN, PENNSYLVANIA 15122-0079

Operated for the U.S. Department of Energy
by WESTINGHOUSE ELECTRIC CORPORATION

DISCLAIMER

Electrical and Optical Performance Characteristics of 0.74eV p/n InGaAs Monolithic Interconnected Modules

David M. Wilt, Navid S. Fatemi[1], Philip P. Jenkins[1], Victor G. Weizer
Richard W. Hoffman, Jr.[1], Raj K. Jain[2], Christopher S. Murray[3] and David R. Riley[3]

NASA Lewis Research Center
Cleveland, Ohio

[1]Essential Research, Inc.
Cleveland, Ohio

[2]National Research Council

[3]Westinghouse Electric Corporation
West Mifflin, PA

Abstract

There has been a traditional trade-off in thermophotovoltaic (TPV) energy conversion development between system efficiency and power density. This trade-off originates from the use of front surface spectral controls such as selective emitters and various types of filters. A monolithic interconnected module (MIM) structure has been developed which allows for both high power densities and high system efficiencies. The MIM device consists of many individual indium gallium arsenide (InGaAs) cells series-connected on a single semi-insulating indium phosphide (InP) substrate. The MIM is exposed to the entire emitter output, thereby maximizing output power density. An infrared (IR) reflector placed on the rear surface of the substrate returns the unused portion of the emitter output spectrum back to the emitter for recycling, thereby providing for high system efficiencies.

Initial MIM development has focused on a 1 cm^2 device consisting of eight (8) series interconnected cells. MIM devices, produced from 0.74eV InGaAs, have demonstrated V_{oc} = 3.2 volts, J_{sc} = 70 mA/cm^2 and a fill factor of 66% under flashlamp testing. Infrared (IR) reflectance measurements (> 2 μm) of these devices indicate a reflectivity of > 82%. MIM devices produced from 0.55eV InGaAs have also been demonstrated. In addition, conventional p/n InGaAs devices with record efficiencies (11.7% AM0) have been demonstrated

Introduction

In thermophotovoltaic (TPV) energy conversion, an emitter is heated to incandescence and a photovoltaic device is placed in view of the emitter to convert the radiant energy into electrical energy. Research in TPV has been renewed recently due to the development of new emitter, filter and photovoltaic cell technologies [10]. Most current efforts in TPV research have concentrated on using front surface spectral control elements such as selective emitters [1] or graybody emitters combined with plasma, dielectric or dipole filters [2,3] in order to improve system efficiency to the 20-40% range predicted by theory.

The front-surface spectral control approach generally produces systems with low power densities (W/cm^2). Selective emitters, for example, have demonstrated in-band emittances ranging from 0.7 to 0.8 [4], with efficiencies of ~40% (i.e. 40% of the emitted energy is convertible by the photovoltaic device). In order to recuperate the non-convertible energy,

3rd NREL TPV CONF - 1997

filters are used to reflect the long-wavelength photons back to the selective emitter. Unfortunately, there are no filters available which provide both 100% transmission in the usable wavelength region and 100% reflection elsewhere. Thus, a selective emitter emittance of 0.8 coupled with a typical filter transmission of 80% leads to a reduction in the power density of 36%. This is an expensive loss, particularly given the cost of TPV cells. A graybody-emitter based system using the same filter would show a similar, although smaller reduction in power density.

A different approach involves the use of rear-surface spectral controls. Using this technique, the entire radiant output from the emitter is incident upon the photovoltaic (PV) device, thereby providing high output power densities. Photons which the PV device is unable to convert, pass through the cell structure and reflect off of a rear reflector back to the emitter for recycling. Researchers have developed TPV cells which utilize low-doped substrates and reflective rear contacts to provide photon recycling [5,6]. Other researchers have developed series-interconnected, monolithic cells for laser, fiber-optic and TPV applications [7,8]. We are developing a cell which combines the advantages of both of these approaches [11].

The Monolithic Interconnected Module or MIM consists of series-connected indium gallium arsenide (InGaAs) devices on a common, semi-insulating indium phosphide (InP) substrate (figure 1). An infrared reflector is deposited on the rear surface of the InP substrate to reflect photons back toward the front surface of the cell. This provides a second pass opportunity for photons capable of being converted by the cell. In addition, long wavelength photons are returned to the emitter for "recycling", improving the system efficiency.

The MIM design offers several advantages. Firstly, small series-connected cells provide high voltages and low currents, reducing I^2R losses. In addition, the small size of the cells permits an array to be comprised of series/parallel strings rather than a single series-connected string of larger cells. This should improve the reliability of the TPV module since the failure of a single cell would not debilitate the entire array. In addition, the cell size and distribution may be easily adjusted to minimize the losses associated with emitter non-uniformity (i.e. variation in view factor, temperature, etc.).

Secondly, the MIM design maximizes output power density since losses associated with front-surface spectral controls are eliminated. This represents a significant simplification of TPV system design and thermal management since there are no filters to cool. Thirdly, the rear surface of the device is not electrically active, therefore the cell may be directly bonded to the substrate/heat sink without concern for electrical isolation. This greatly simplifies the array design and improves the thermal control of the cells. Lastly, photons which are weakly absorbed have the possibility of multiple passes through the cell structure. This feature is particularly important for lattice-mismatched devices, where poor minority carrier diffusion length can be partially offset by making the cell thin, forcing the carrier generation to occur closer to the p/n junction.

Although the MIM design has many beneficial attributes, there are limitations. The device is produced on an InP substrate using organo metallic vapor phase epitaxy (OMVPE) growth techniques and as such may be too expensive for many commercial applications. The simplification of array fabrication may partially offset the higher cost of the MIM's compared to conventional TPV devices.

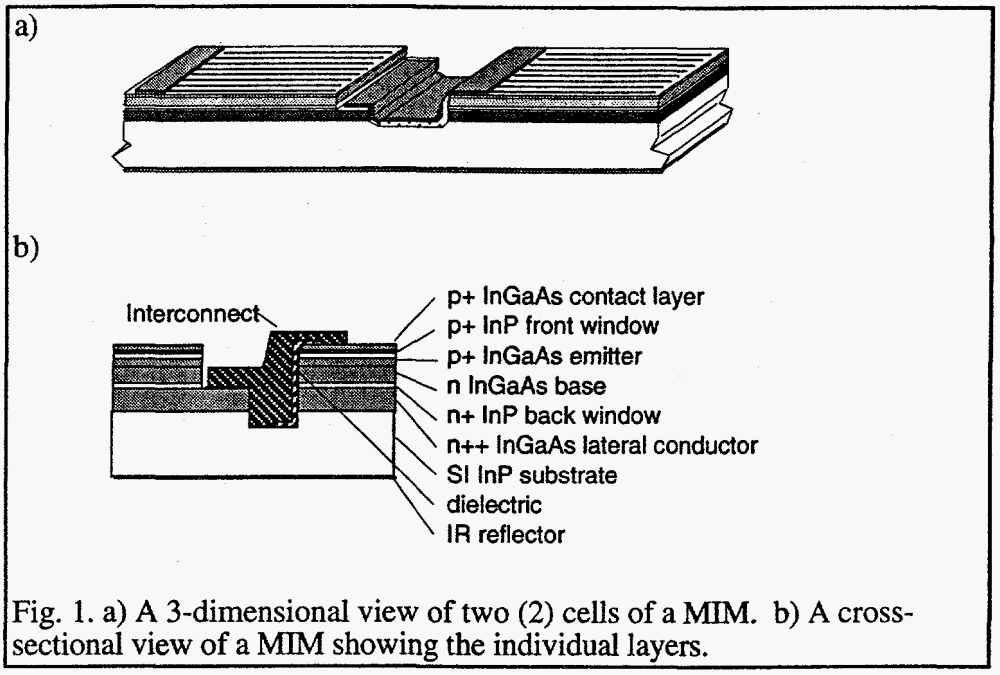

Fig. 1. a) A 3-dimensional view of two (2) cells of a MIM. b) A cross-sectional view of a MIM showing the individual layers.

MIM Development

Optical Development

Successful development of the MIM device requires balancing trade-offs between optical performance (mid IR reflectivity) and electrical performance. To address the optical performance issues, the free carrier absorption (FCA) for both n and p-type InGaAs as a function of dopant type, level, thickness and wavelength was determined. Calibration samples with doping levels ranging from 5e18 to 3e19 cm^{-3} were fabricated on semi-insulating InP substrates. Absorption measurements were conducted using a spectrophotometer for the near IR (1 - 3 μm) and a FTIR for the mid IR (3 - 10 μm). The spectrophotometer data (fig. 2) was fitted to determine the actual absorption for a single pass through the material (i.e. the measured data was corrected for reflection off of the surface, epi/substrate interface and the back substrate/air interface). The corrected data was fitted to the following equation:

$$\text{absorption}(\lambda) = 1 - \exp(-\alpha(\lambda) * t) \quad (1)$$

where: $\alpha(\lambda) = (C(\lambda) * n)$ for n-type material (2)

$\alpha(\lambda) = (C(\lambda) * p)$ for p-type material (3)

n = electron (doping) density (cm^{-3})
p = hole (doping) density (cm^{-3})
t = thickness in cm

The analysis indicates that for an equivalently doped InGaAs layer, the p-type material will have a FCA (averaged from 1.9 to 3 microns) 17x higher than the equivalently doped n-type material (C = 7.97e-17 for p-type InGaAs, C = 4.48e-18 for n-type InGaAs). This is an important consideration when determining the optimum polarity of the MIM device.

Another interesting feature of the absorption measurements is the shift in apparent bandgap (0.3eV) for the heavily doped n-type InGaAs. We have determined that this shift is caused

by a Burstein-Moss shift in the degenerately doped material. The use of this material as the

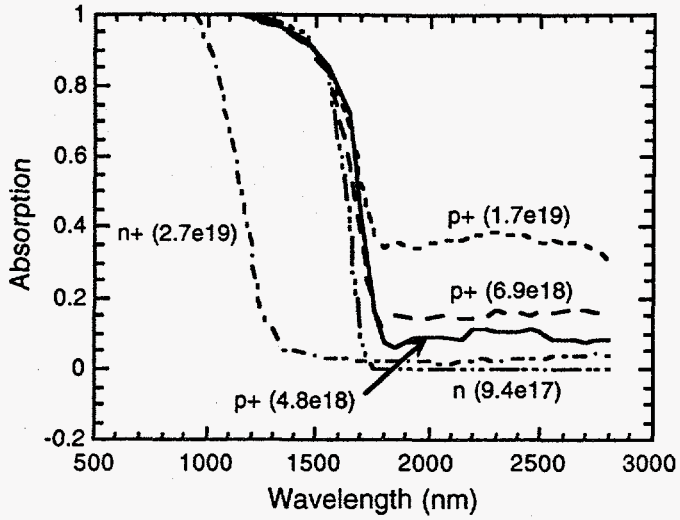

Figure 2 - Absorption measurements for 3μm thick 0.74eV InGaAs layers with various doping levels.

lateral conduction layer (LCL) (fig.1) allows the base of the cell to be thinned for incomplete absorption. Photons which are not absorbed in the cell on the first pass are able to pass through the LCL, bounce off of the back surface reflector (BSR) and have a second pass through the cell. This approach may not be optimal for 0.74eV material where the FCA in the n++ LCL represents a significant loss (3.6% absorption/pass for 3μm LCL) with only a minor benefit to the device performance. The technique may be best applied to lattice-mismatched material which suffers from poor minority carrier lifetimes in the base, where reducing the base thickness should increase the current as well as the voltage.

The FTIR data indicated that the n-type material has low absorption up to the plasma frequency which shifts from 7 microns to 12 microns as the doping density is varied from 3e19 to 8e18 cm^{-3}. The choice of doping density represents another trade-off between FCA and resistive losses. At this point of the MIM development, we are focusing on the electrical development and will address the optimization with respect to optical performance once the fabrication process is well established. The other elements of the optical performance, such as BSR and contact reflectivity and anti-reflection coating development, are covered in a related paper presented at this conference [9].

Electrical Development

The MIM device is currently being developed for use with a low temperature (1200K) blackbody emitter. Assuming a quantum efficiency of 1 and a view factor of 1, a 0.74eV device would produce a Jsc of 0.87 A/cm^2 and a 0.55eV device would produce 3.72 A/cm^2. Based on these current densities, cell structures were determined which limit the resistive losses in the LCL and emitter to 1% for each layer. The device structures are shown in figure 3.

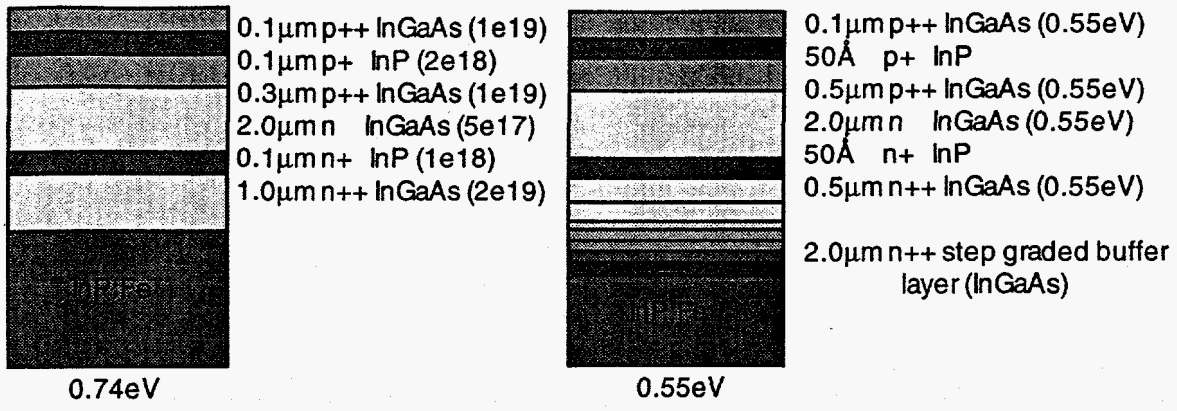

Figure 3 - 0.74 and 0.55eV device structures for operation with a 1200K blackbody.

The thin (0.1 micron) p++ InGaAs top layer was added as a contact layer so that non-alloyed ohmic contacts could be used for both the emitter and base contacts. The InGaAs contact layer was removed from between the grid fingers after metallization.

The MIMs reported in this paper were all fabricated as 1 cm^2 devices consisting of eight (8) cells with 300 micron interconnects and 7 micron grid fingers on 100 micron centers. Subsequent processing developments have reduced the interconnect width to 50 microns and the grid finger widths to 5 microns [9]. Using these dimensions, a new mask set has been developed to produce 5mm x 5mm MIMs consisting of eight (8) 500 micron wide cells with the 50μm interconnects. Test structures have been successfully processed with this design although the results will be presented at a later date.

Results

Conventional planar p/n InGaAs devices were produced using the active cell layers shown in figure 2a (note: the emitter doping was reduced to 1e18 cm^{-3} for these devices) in order to verify the basic material quality. The I-V curve shown in figure 4 demonstrates the quality of the baseline devices. The efficiency (11.7% AM0) represents a record for 0.74eV p/n InGaAs. Calculations indicate that reducing the grid shadowing from the 16% on the test device to the 5% normally used in AM0 devices would increase the efficiency to >13%, a record for any 0.74eV InGaAs device (p/n or n/p).

The external quantum efficiency for a 0.74eV baseline device with a dual layer anti-reflective coating is shown in figure 5. As was stated earlier, the base region was intentionally grown thin so that the effect of the BSR would be demonstrated. It was initially puzzling to observe the high bandedge photoresponse from the conventional cell (with no BSR). Optical modeling indicates that only 62% of the bandedge photons (1600nm) are absorbed in the thin base region, assuming a single pass. Thus, the internal QE could not be greater than 62%. At 1600nm the baseline device demonstrated a 74% internal QE (66% external QE, 10% reflection). The transmission characteristic of a n+ InP substrate was measured at 1600nm and indicated >45% transmission (not corrected for absorption and reflection). Thus bandedge photons which are not absorbed in the cell are able to reach the back contact, which is a very reflective non-alloyed Au based contact. It is believed that this contact acts as a BSR, reflecting the bandedge photons back toward the active cell region. Our past p/n devices had all utilized a sintered contact which forms a highly absorbing Au_2P_3 compound at the semiconductor/metal interface. The QE characteristics of these devices did not demonstrate this enhanced bandedge photoresponse.

To test this theory, p/n planar cells were fabricated from the same epitaxial InGaAs material with and without sintered back contacts. The QE test data confirmed the reduction in long wavelength response with sintered back contacts compared to non-alloyed contacts.

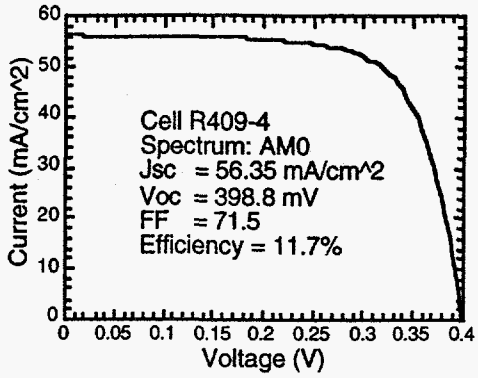

Figure 4 - AM0 I-V characteristic of 0.74eV baseline p/n InGaAs device.

A negative aspect of this feature is that the reflection is diffuse in nature. Thus non-convertible photons may be totally internally reflected and add to the thermal load of the cell. A benefit of the diffuse reflection is that convertible photons will generally have a longer path length in the active cell layers, improving the probability for absorption. Given the high absorption coefficient for InGaAs, this is a marginal benefit.

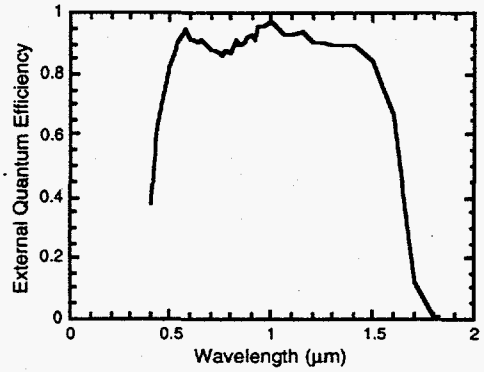

Figure 5 - External QE of 0.74eV p/n baseline structure with dual AR

The I-V curve for a 0.74eV MIM device is shown in Figure 6 under flashlamp testing. The data indicates an average voltage of 400 mV per cell. This particular device was produced prior to the development of the high quality Si_3N_4 dielectric and therefore is not expected to demonstrate optimum performance. The I-V characteristics of individual cells were examined and found to vary greatly within a single MIM device. The cell characteristics ranged from high quality diodes to heavily shunted or even shorted devices. We believe that this variation is caused by defects in the dielectric isolation layer and/or particulate related defects in the epitaxial material. Again, all of these devices were produced prior to the optimization of the Si_3N_4 layer and were also produced during a major building rehab

which was the source of the particulate contaminates in the epitaxial material. We have observed that if a grid finger covers a particulate damaged region, the device shows a shunt characteristic. Although, if the problem area is removed by cleaving, the device performance is significantly improved.

The external QE curve for the 0.74eV device is shown in figure 7 (without an anti-reflective coating). The QE data represents the aggregate worst response from across the entire device, given the series interconnected nature of the MIM design. This device is expected to produce 48.5 mA when illuminated by a 1200K blackbody emitter with a view factor of 1.

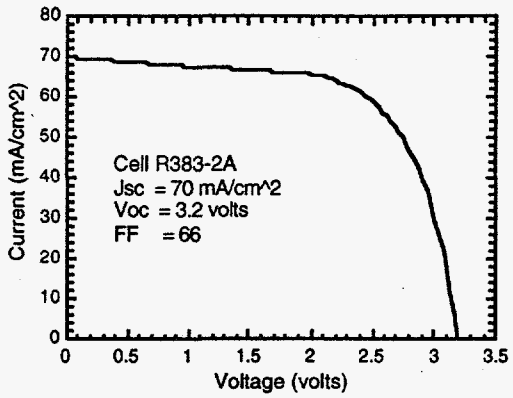

Figure 6 - I-V characteristic of 0.74eV MIM under flashlamp testing.

A 0.55eV MIM was produced to determine if there were any unforeseen difficulties or problems in producing a MIM from lattice mismatched material. Figure 8 shows the I-V characteristic of a 0.55eV MIM under AM0 testing. As with the 0.74eV device reported above, this cell was produced prior to the optimization of the dielectric material. Unfortunately, this device was destroyed prior to I-V testing at higher injection levels.

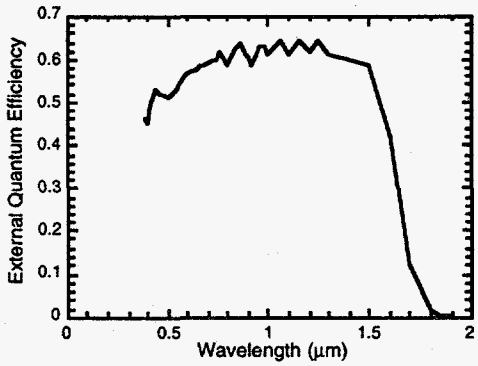

Figure 7 - External QE of 0.74eV MIM (no AR).

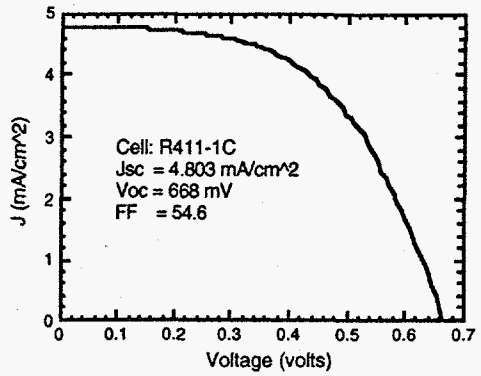

Figure 8 - AM0 I-V characteristic of 0.55eV MIM device (no AR)

Figure 9 shows the external QE characteristic for the 0.55eV MIM (without AR). Given the rudimentary nature of the buffer layer used to produce this device and the limited development of the cell layers, the results were very promising.

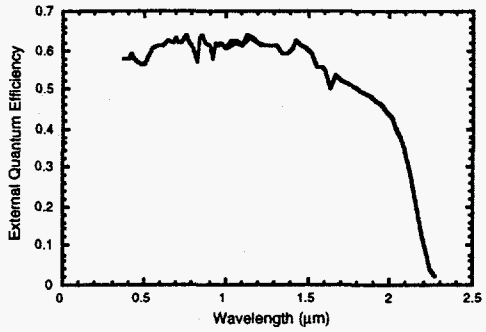

Figure 9 - External QE of 0.55eV MIM (no AR)

Figure 10 shows the measured reflectivity for a 0.74eV MIM device (without an AR coating). This particular device had a 3μm LCL and a low doped emitter (1e18 cm^{-3}). Optical modeling suggests that IR reflectivity's of >90% are possible with optimized device structures.

Acknowledgment

The authors wish to acknowledge Dave Scheiman of NASA LeRC for the I-V and QE measurements.

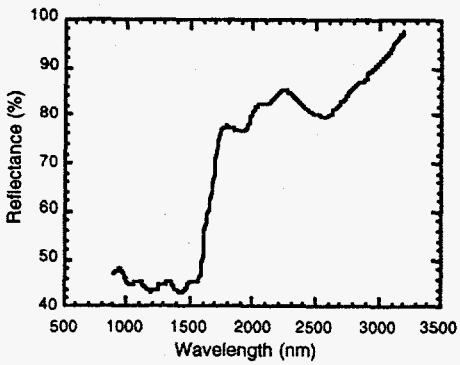

Figure 10 - Reflectance of 0.74eV MIM (no AR)

REFERENCES

[1] D.L. Chubb and R.L. Lowe, "Thin-Film Selective Emitter", J. Appl. Phys. **79** (9), 1993, pp. 5687-5698.

[2] D.M. Wilt et al., "InGaAs PV Device Development for TPV Power Systems", 1st NREL Conf. on TPV Gen. of Elect., 1994, AIP 321, pp. 210.

[3] W.E. Horne et.al., "IR Filters for TPV Convertor Modules", Proc. 2nd NREL Conf. on TPV Gen. of Elect., 1995, AIP 358, pp. 35.

[4] D.L Chubb et.al., "Review of Recent TPV Research at Lewis Research Center", Proc. 14th SPRAT Conf, 1995, NASA CP-3324, pp. 191.

[5] G.W. Charache et.al., "Thermophotovoltaic Devices Utilizing a Back Surface Reflector for Spectral Control", Proc. 2nd NREL Conf. on TPV Gen. of Elect., 1995, AIP 358, pp. 339.

[6] P.A. Iles and C.L. Chu, "TPV Cells with High BSR", Proc. 2nd NREL Conf. on TPV Gen. of Elect., 1995, AIP 358, pp. 361.

[7] S. Wojtczuk, "Multijunction InGaAs Thermophotovoltaic Power Convertor", Proc. 14th SPRAT Conf, 1995, NASA CP-3324, pp. 223.

[8] M.B. Spitzer et.al., "Monolithic Series-Connected Gallium Arsenide Convertor Development", Proc. IEEE 22nd PVSC, (1991), pp. 142-146.

[9] N.S. Fatemi, et al., "Materials and Process Development for the Monolithically Interconnected Module (MIM) InGaAs/InP TPV Cells", Proc. 3rd NREL Conf. on TPV Generation of Electricity, 1997.

[10] D.M. Wilt, et al., "High Efficiency InGaAs Photovoltaic Devices for TPV Power Systems", Appl. Phys. Lett. **64** (18), 1994.

[11] D.Wilt, et al,"Monolithically Interconnected InGaAs TPV Module Development", Proc. IEEE 25th PVSC, May 1996, pp.43